Solid-State Electronics, 1978, Vol. 21, pp. 107–114. Pergamon Press. Printed in Great Britain

ALLOY SCATTERING AND HIGH FIELD TRANSPORT IN TERNARY AND QUATERNARY III–V SEMICONDUCTORS†

M. A. LITTLEJOHN, J. R. HAUSER and T. H. GLISSON
Electrical Engineering Department, N.C. State University, Raleigh, NC 27607, U.S.A.

and

D. K. FERRY
Office of Naval Research, Arlington, VA 22217, U.S.A.

J. W. HARRISON
Research Triangle Institute, Research Triangle Park, NC 27709, U.S.A.

Abstract—A technique is described for the estimation of the influence of random potential alloy scattering on the high field transport properties of quaternary III–V semiconductors obtained by Monte Carlo simulation. The approach is based on an extension of a theoretical model for scattering in the ternary alloys. The magnitude of the scattering potential is an important parameter in alloy scattering, and three proposed models for calculating this potential are discussed. These are the energy bandgap difference, the electron affinity difference, and the heteropolar energy difference for the appropriate binary compounds.

The technique is used in the Monte Carlo method to study the influence of alloy scattering on the transport properties of III–V quaternary alloys. The results of this study are used in a device model to estimate device parameters for FETs.

INTRODUCTION

In a semiconductor solid solution alloy, the scattering of free carriers due to the deviations from the perfect periodicity of the virtual crystal model, originally conceptualized by Nordheim[1], can be called random potential alloy scattering. The discussion of alloy scattering in relation to experimental electron mobility in III–V semi-conductor ternary alloys has been based on an unpublished result of Brooks[2], as quoted and used for example in the results of Tietjen and Weisberg[3], Makowski and Glicksman[4], Glicksman *et al.*[5], and Takeda *et al.*[6]. Recently, theoretical calculations[7, 8] have elaborated on physical models for alloy scattering in ternary III–V semiconductors, and these models have been applied in the Monte Carlo method to include the effects of alloy scattering in high field transport calculations for $InP_{1-x}As_x$ ternary alloys[9] and $Ga_{1-x}In_xP_{1-y}As_y$ quaternary alloys[10].

The III–V quaternary semiconductor alloys are becoming of great technological importance, and offer for device applications the unique feature that the energy band gap can be varied while maintaining a fixed lattice constant[11] by varying the alloy composition. It is important in these materials to be able to estimate the influence of alloy scattering on the electronic transport properties. The Monte Carlo method[12] is one of the more reliable techniques for making such an estimate, and this technique does become a predictive tool for III–V ternary and quaternary materials as long as reliable material property data are available for the binary constituents[7–10].

†This work was supported by research contract No. N00014-70-A-0120-004 from the Office of Naval Research, Arlington, VA, and by research contract No. F33615-76-C-1265 from the Air Force Avionics Laboratory, Wright Patterson AFB, Ohio.

The purpose of this paper is to present a technique for estimating the effect of alloy scattering on transport properties of III–V ternary and quaternary semiconductors. This procedure has been used previously[9, 10], and will be discussed in detail in this paper. The results obtained from the method applied in Monte Carlo transport calculations are also used to predict the influence of alloy scattering on device performance. The intent is to establish some reasonable upper- and lower-bounds for the effect of this scattering process in the ternary and quaternary materials.

TERNARY ALLOY SCATTERING POTENTIAL

The electron scattering rate in ternary semiconductors due to alloy scattering is important for the development of the quaternary scattering rate. Of particular importance is the scattering potential used in this calculation. The scattering rate (transition probability) for a ternary alloy ($A_{1-x}B_xC$) with nonparabolic energy bands is given in r.m.k.s. units by[7–9].

$$\frac{1}{\tau_{TA}} = \frac{3\pi}{8\sqrt{(2)}} \frac{(m^*)^{3/2}}{\hbar^4} [x(1-x)]\gamma(\epsilon) \frac{d\gamma(\epsilon)}{d\epsilon} \Omega |\Delta U|^2 S(\alpha) \tag{1}$$

where the notation used is described in Ref.[10]. Here $S(\alpha)$ is an energy-dependent parameter which describes the effect of ordering on the scattering rate[13]. In general, $0 \leq S \leq 1$, where $S = 0$ for a perfectly ordered ternary (superlattice) and $S = 1$ for a completely random alloy. The evaluation of S is complex and depends on the scattering potential, ΔU. In this paper the two cases $S = 0$, 1, along with different scattering potentials for the case $S = 1$, will be used to give lower- and upper-bound effects of alloy scattering, according to results obtained from the Monte Carlo method.

Besides the effect of ordering, the most significant parameter in eqn (1) is the scattering potential, ΔU. The derivation of eqn (1) is based on the Mott-inner potential[8], since this potential results in a relaxation time which leads to the accepted temperature dependence of electron mobility due to alloy scattering[5, 7]. Previous calculations have used either (a) the difference in energy band gaps between the binary constituents[2–6], or (b) the difference in electron affinities between the binary constituents[7–10] for this scattering potential.

Recently, Ferry[14] has suggested another form for the scattering potential based on the electronegativity theory of Phillips[15]. In this work, the energy difference between the bonding and antibonding hybridized molecular (sp^3) orbitals of a tetrahedrally coordinated crystal can be decomposed into contributions due to symmetric and antisymmetric potentials within a unit cell. This relation is described by[15]

$$E_G^2 = E_H^2 + C^2 \tag{2}$$

where E_G is the energy difference between the bonding and antibonding molecular states, E_H is the homopolar (symmetric) part and C is the heteropolar (antisymmetric) part of this energy difference. The heteropolar energy C represents the charge transfer or ionic contribution to E_G, and if in the alloy all bond lengths are equal, then it can be assumed that any fluctuations in the crystal potential arise from fluctuations in C[16]. This approach has had some limited success in explaining energy bandgap "bowing" effects in ternary semiconductors[16, 17].

In Appendix A an expression for the scattering potential in a ternary alloy $A_{1-x}B_xC$ based on the electronegativity theory is given[14]. This expression is

$$\Delta U_{EN} = \frac{bZ}{4\pi\epsilon_0}\left[\frac{1}{r_A} - \frac{1}{r_B}\right]\exp\left[-k_s R_A\right] \tag{3}$$

Each quantity in this expression is defined in Appendix A.

Table 1 lists values of ΔU_{EN} for several ternary III–V alloys, along with ΔU_{EG}, the energy gap difference, and ΔU_{EA}, the electron affinity difference. The values of ΔU_{EN} are given in Table 1 for $x = 0.5$, since there is a slight functional dependence of ΔU_{EN} on the alloy composition x. This is illustrated in Fig. 1 where the compositional dependence of ΔU_{EN} is shown for several ternary alloys.

Figure 2 shows the effect of the use of these three scattering potentials on the velocity field characteristics for $Ga_{0.5}In_{0.5}As$ obtained from Monte Carlo calculations. Also shown in this figure is the characteristic for $S = 0$ (no alloy scattering), and the curve for GaAs for comparison. These calculations have used the $\Gamma - L - X$ conduction band ordering proposed for GaAs by

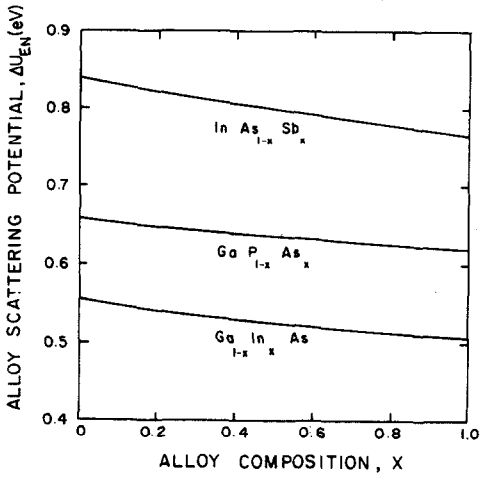

Fig. 1. Electron scattering potential for ternary alloys obtained from the heteropolar energy difference of the binary constituents.

Table 1. Alloy scattering potentials in electron volts for several ternary III–V semiconductors for (a) the electronegativity theory (ΔU_{EN}) (b) the electron affinity difference (ΔU_{EA}) (c) the energy band gap difference (ΔU_{EG})

Material	a) $\Delta U_{EN}(x=0.5)$	b) ΔU_{EA}	c) ΔU_{EG}
$Ga_{1-x}In_xAs$	0.529	0.830	1.08
$InP_{1-x}As_x$	0.581	0.50	0.981
$GaP_{1-x}As_x$	0.637	0.07	1.30
$InAs_{1-x}Sb_x$	0.801	0.310	0.184
$Al_{1-x}In_xAs$	0.466	1.320	1.790
$AlP_{1-x}As_x$	0.636	0.08	0.267
$Ga_{1-x}In_xP$	0.559	0.40	0.92
$Al_{1-x}In_xP$	0.541	0.90	1.08
$Ga_{1-x}In_xSb$	0.486	0.53	0.515
$InP_{1-x}Sb_x$	1.32	0.19	1.165
$GaP_{1-x}Sb_x$	1.51	0.06	1.57

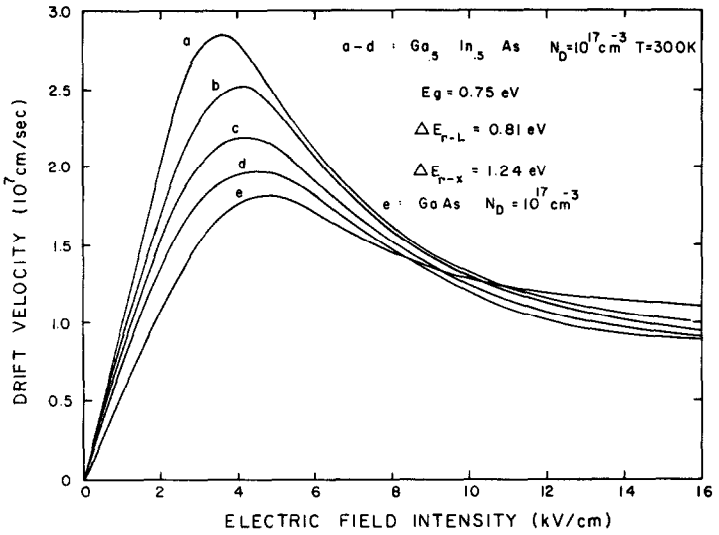

Fig. 2. Velocity-field characteristic for $Ga_{0.5}In_{0.5}As$ obtained by Monte Carlo simulation. The notation is: Curve (a) No alloy scattering $\mu = 9700\,cm^2/V \cdot sec$; Curve (b) Calculated using ΔU_{EN}, $\mu = 8600\,cm^2/V\,sec$; Curve (c) Calculated using ΔU_{EA}, $\mu = 8300\,cm^2/V\,sec$; Curve (d) Calculated using ΔU_{EG}, $\mu = 7350\,cm^2/V\,sec$; Curve (e) GaAs, $N_D = 10^{17}\,cm^{-3}$, $\mu = 4900\,cm^2/V\,sec$. Note: For $Ga_{0.47}In_{0.53}As$ at $T = 300\,K$, $\mu = 8450\,cm^2/V\,sec$ [Ref. [6]].

Aspnes[18], and GaAs material parameters resulting in a good fit to experimental data[19]. Also given in Fig. 2 is a tabulation of the low-field electron mobility for each scattering potential. In the recent work of Takeda *et al.*[6] the experimental Hall mobility for $Ga_{0.47}In_{0.53}As$ in $8450\,cm^2/V\,sec$. The Monte Carlo drift mobilities calculated by the maximum likelihood estimation technique[9, 10] are $7350\,cm^2/V\,sec$, $8300\,cm^2/V\,sec$, and $8900\,cm^2/V\,sec$ using ΔU_{EG}, ΔU_{EA} and ΔU_{EN}, respectively, in the calculations. In general, the Hall mobility is greater than the drift mobility, so that based on these low field mobility calculations the scattering potential is possibly closer to that predicted by the electron affinity difference for this material.

If one examines the trends for the eighteen possible III–V ternary alloys it appears that often $\Delta U_{EN} < \Delta U_{EA} < \Delta U_{EG}$. However, this is not always true, as can be seen by the examples chosen for Table 1. At best, this ordering of the ΔU's seems fortuitous, and the ordering between ΔU_{EN} and ΔU_{EA} is especially in question. The band gap differences are the most accurately known parameters, while there are uncertainties in the available values of electron affinities[20] and covalent radii[21]. Thus the ordering in Table 1 could be the result of experimental variations, especially between the ΔU_{EN} and the ΔU_{EA}. At the present time there are no firm theoretical or experimental reasons for choosing either scattering potential to evaluate the scattering rate due to alloy scattering in the ternaries. The point to be made is that alloy scattering as used in the Monte Carlo method and based on eqn (1) has a very detrimental effect on the transport properties of III–V ternary alloys and thus will be a factor in their use in devices, if the proposed models are correct.

QUATERNARY ALLOY SCATTERING RATE

Appendix B develops an extension of the ternary alloy scattering rate model to a quaternary material, $A_{1-x}B_xC_{1-y}D_y$, where A and B are group III atoms and C and D are group V atoms. This relation, which applies to the case where the A and B atoms are randomly distributed on the group III sites and the C and D atoms are randomly distributed on the group V sites, is given by

$$\frac{1}{\tau_{QA}} = K|\Delta U_Q(x, y)|^2, \tag{4}$$

where

$$K = \frac{3\pi}{8\sqrt{(2)}} \frac{(m^*)^{3/2}}{\hbar^4} \gamma(\epsilon) \frac{d\gamma(\epsilon)}{d\epsilon} \Omega,$$

and

$$\begin{aligned}|\Delta U_Q(x, y)|^2 = {} & x(1-x)y^2|\Delta U_{ABD}|^2 \\ & + x(1-x)(1-y)^2|\Delta U_{ABC}|^2 \\ & + y(1-y)x^2|\Delta U_{BCD}|^2 \\ & + y(1-y)(1-x)^2|\Delta U_{ACD}|^2.\end{aligned}$$

Here the effective mass, m^*, and the primitive cell volume, Ω, are calculated according to an interpolation procedure described previously[10].

Table 2 lists the quaternary alloy scattering potential ΔU_{QA} of eqn (4) at the mid-composition range $x = y = 0.5$ for three quaternary alloys, $Ga_{1-x}In_xP_{1-y}As_y$, $Ga_{1-x}In_xP_{1-y}Sb_y$, and $Al_{1-x}In_xP_{1-y}As_y$ for each of the three ternary scattering potentials described in the last section. When comparing the results of Tables 1 and 2, the numbers given in Table 1 should be divided by 1/4 since the factor $x(1-x)$ in eqn (1) is not included in the Table 1 entries, whereas the analogous factor is included in the entries of Table 2. In general, the quaternary scattering potential (not the scattering rate) is larger than

Table 2. Quaternary alloy scattering parameter in electron volts for quaternary III–V semiconductors for (a) the electronegativity theory (ΔU_{EN}) (b) the elctron affinity difference (ΔU_{EA}) (c) the energy gap difference (ΔU_{EG}). The composition is chosen as $x = y = 0.5$ for convenience

Material	a) $\Delta U_{QA}(\Delta U_{EN})$	b) $\Delta U_{QA}(\Delta U_{EA})$	c) $\Delta U_{QA}(\Delta U_{EG})$
$Ga_{1-x}In_xP_{1-y}As_y$	0.289	0.263	0.540
$Ga_{1-x}In_xP_{1-y}Sb_y$	0.536	0.173	0.555
$Al_{1-x}In_xP_{1-y}As_y$	0.280	0.419	0.581

the scattering potential for any of the four ternaries of which the quaternary is composed.

Figure 3 shows a plot of the quaternary alloy scattering parameter surface (ΔU_{QA}^2) for $Ga_{1-x}In_xP_{1-y}As_y$ in the compositional plane ($0 \le x \le 1, 0 \le y \le 1$) for the case where the ternary scattering potentials are taken as the electron affinity differences. This figure shows a relative minimum of the quaternary alloy scattering parameter, ΔU_{QA}^2, along a region which is very close to the compositions required for lattice matching this quaternary to InP substrates. This contributes to the large predicted peak velocity[10] of this particular quaternary alloy matched to InP. However, if the energy gap difference is used for the scattering potential the shape of the curve is shifted to a less favorable situation for minimum alloy scattering using InP as a substrate. Also, for compositions away from this region of minimum alloy scattering, the effects of alloy scattering are more detrimental. This can be seen in Fig. 4, where the velocity-field characteristic for $Ga_{0.55}In_{0.45}P_{0.1}As_{0.9}$ are shown. Without alloy scattering these characteristics are nearly as attractive for device applications as those previously reported for $Ga_{0.27}In_{0.73}P_{0.4}As_{0.6}$. However, alloy scattering has a much more detrimental effect on the velocity-field curves for this particular composition. Also, for the composition shown in Fig. 4, the effect of alloy scattering due to the use of ΔU_{EN} and ΔU_{EA} are almost identical, and only one velocity-field curve is shown for the calculations made from each of these alloy scattering potentials.

Other different effects of alloy scattering in quaternary alloys are illustrated in the velocity-field characteristics shown in Figs. 5 and 6 for $Al_{0.25}In_{0.75}P_{0.25}As_{0.75}$ and $Ga_{0.25}In_{0.75}P_{0.84}Sb_{0.16}$, respectively. Since out interest in these materials has been primarily for FET's, the velocity-field curves are given for a doping level of $10^{17}\,cm^{-3}$. It is seen that when alloy scattering is not used in the Monte Carlo simulations, the general features of these velocity-field curves are most attractive for a wide variety of solid state Gunn-effect electronic devices[24]. These features include large low-field mobility, high peak velocity, low threshold field, large energy band gap, large intervalley energy band separation, large negative differential mobility, and large peak-to-valley drift velocity ratio. When alloy scattering is included, its effects are generally detrimental to all these desirable properties. The extent of this degradation is certainly open to question, although the use of Monte Carlo method with the present alloy scattering model can provide a very good estimation of the range of this degradation.

At the same time the results of the Monte Carlo analysis can be used in device models to estimate device figures-of-merit and to examine their degradation from alloy scattering. This is illustrated in Table 3, where the FET model of Lehovec and Zuleeg[25] has been used to calculate some device parameters for MESFETs using

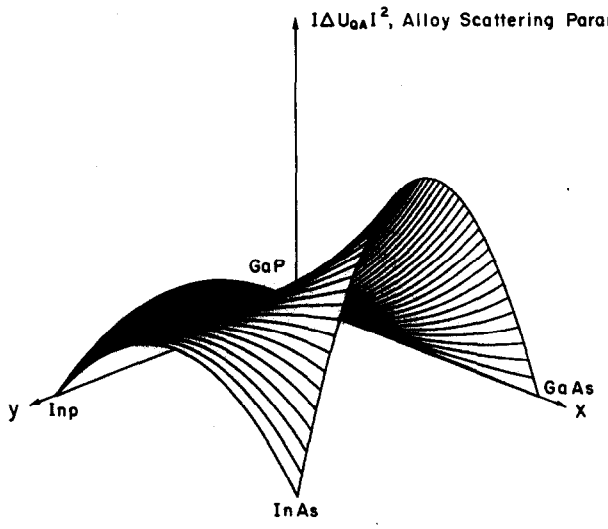

Fig. 3. Quaternary alloy scattering parameter, $|\Delta U_{QA}|^2(eV^2)$, for $Ga_{1-x}In_xP_{1-y}As_y$.

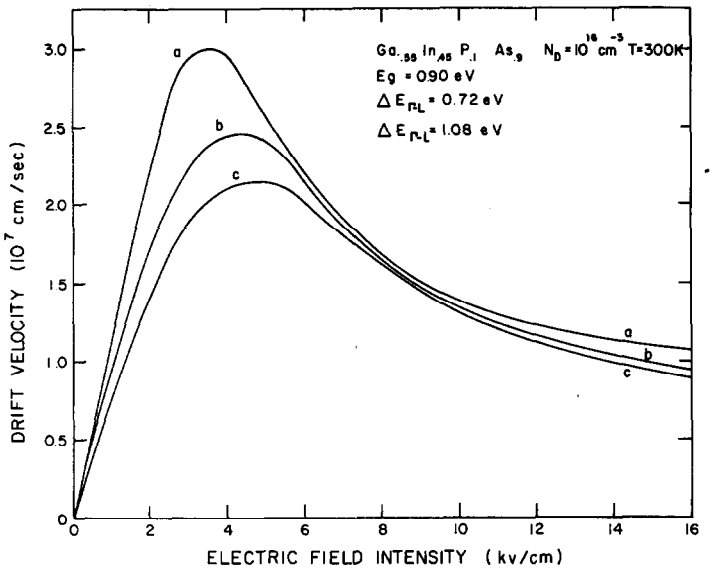

Fig. 4. Velocity-field characteristic for $Ga_{0.55}In_{0.45}P_{0.1}As_{0.9}$ obtained by Monte Carlo simulation. The notation is: Curve (a) No alloy scattering; Curve (b) Calculated using ΔU_{EA} and ΔU_{EN}; Curve (c) Calculated using ΔU_{EG}.

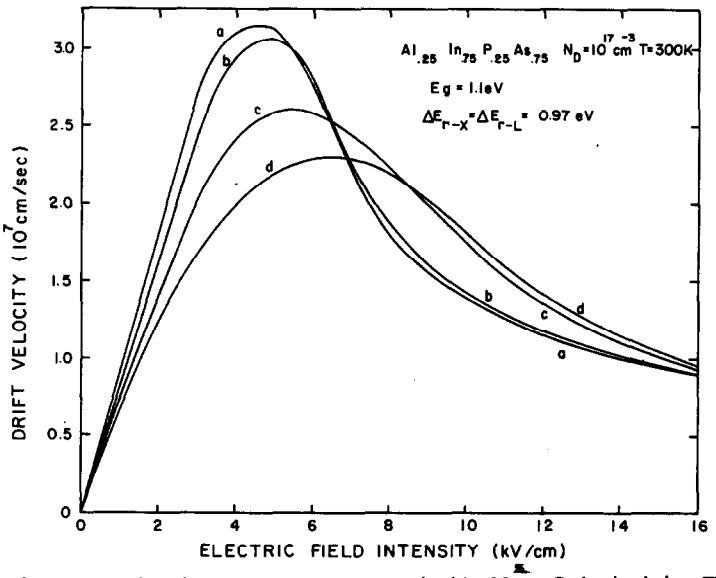

Fig. 5. Velocity-field characteristic for $Al_{0.25}In_{0.75}P_{0.25}As_{0.75}$ obtained by Monte Carlo simulation. The notation is: Curve (a) No alloy scattering; Curve (b) Calculated using ΔU_{EN}; Curve (c) Calculated using ΔU_{EA}; Curve (d) Calculated using ΔU_{EG}.

the ternary and quaternary materials discussed in this paper. While this particular device model includes velocity saturation, but does not include a negative differential mobility, it has recently been used as a design model for GaAs MESFETs[26], with good results. The important comparison to be made is that between the device parameters for GaAs and the ternary and quaternary materials, and to consider the effect of alloy scattering on these device figures-of-merit. These three materials have properties which suggest possible improvements in MESFET performance over GaAs (although the bandgap of 0.8 eV for $Ga_{0.5}In_{0.5}As$ may be somewhat too low), and these first-order model calculations verify this suggestion. Depending on the amount of alloy scattering and the physical correctness of the proposed model, alloy scattering reduces the advantages the materials offer. However, even considering the uncertainty in the magnitude of the alloy scattering the ternary and quaternary device parameters, such as f_T in Table 3, are seen to be improved considerably over the GaAs device parameters.

This paper has presented techniques which can be used in the Monte Carlo method to estimate the effects of random potential alloy scattering on the high field transport properties of ternary and quaternary III–V semiconductors. These materials have many properties

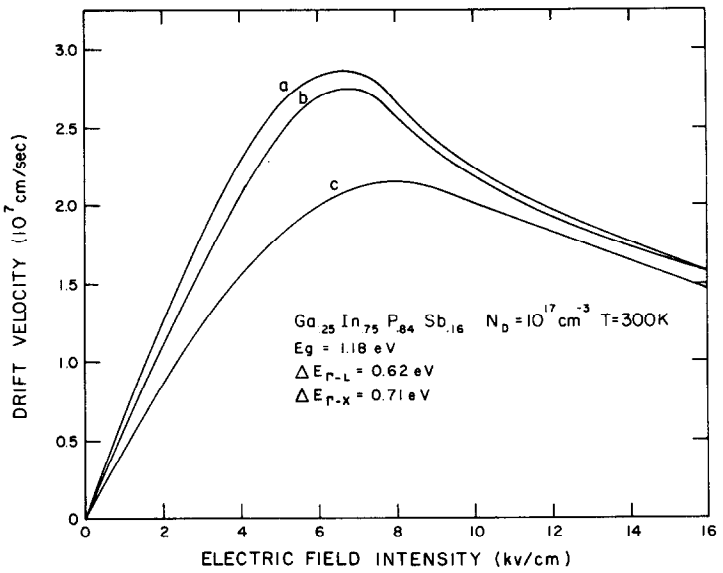

Fig. 6. Velocity-field characteristic for $Ga_{0.25}In_{0.75}P_{0.84}Sb_{0.16}$ obtained by Monte Carlo simulation. The notation is: Curve (a) No alloy scattering; Curve (b) Calculated using ΔU_{EA}; Curve (c) Calculated using ΔU_{EN} and ΔU_{EG}.

Table 3. Field-effect transistor parameters based on the model of Lehovec and Zuleeg[25] for the materials discussed in this paper, illustrating the effect of alloy scattering

Material	g_m(mS)	C_{gs}(pf)	f_T(GHz)	r_{Ds}(ohms)	f_{max}(GHz)	τ_T(psec)
GaAs	30.48	.3640	13.33	445.06	24.55	9.25
$Ga_{.5}In_{.5}As$						
a) No alloy	61.39	.4886	20.00	202.31	35.23	5.79
b) ΔU_{EN}	54.61	.4884	17.79	228.28	31.40	6.51
c) ΔU_{EA}	48.39	.4914	15.67	247.39	27.12	7.39
d) ΔU_{EG}	43.24	.4910	14.02	278.39	24.32	8.27
$Ga_{.25}In_{.75}P_{.84}Sb_{.16}$						
a) No alloy	47.55	.3820	19.81	335.42	39.56	6.12
b) ΔU_{EA}	44.16	.3778	18.60	390.17	38.61	6.64
c) ΔU_{EN}, ΔU_{EG}	35.55	.3811	14.85	456.20	29.89	8.25
$Al_{.25}In_{.75}P_{.25}As_{.75}$						
a) No alloy	57.85	.4073	22.60	235.35	41.70	5.34
b) ΔU_{EN}	56.73	.4082	22.12	236.15	40.47	5.46
c) ΔU_{EA}	47.47	.4059	18.62	294.33	34.79	6.49
d) ΔU_{EG}	42.66	.4101	16.56	303.41	29.78	7.28

Notation: g_m = device transconductance, C_{gs} = gate-source capacitance, f_T = gain-bandwidth product, r_{Ds} = small signal drain-source resistance, f_{max} = maximum frequency of oscillation, τ_T = source-drain transit time.

These calculations were made for a device with a channel doping of $10^{17}cm^{-3}$ and the following dimensions: Channel width = 0.3μm, Channel length = 1.5μm, Channel depth = 300 μm. The gate voltage = 0 volts and the drain voltage equals the pinch-off voltage.

which suggest that their utilization in Gunn-effect electron devices can improve presently achievable device performance. At the same time, the effect of alloy scattering on material properties and characteristics which determine device performance present questions which challenge the extent of this conclusion.

The intent of this paper, and other publications [7–10], has been to offer a reasonable calculation of the effects of alloy scattering on the material and transport properties of ternary and quaternary III–V semiconductors. Of the three methods discussed for estimating the magnitude of the scattering potential, the bandgap difference is probably least accurate. The other two estimations represent two different views of the alloy scattering potential. For some materials the electron affinity difference technique and heteropolar energy difference technique give comparable magnitudes for the scattering potential. For other materials such as $GaP_{1-x}As_x$, $AlP_{1-x}As_x$ and $GaP_{1-x}Sb_x$ the electron affinity difference gives a very small alloy scattering effect while the heteropolar energy difference gives a large alloy scattering effect. Experimental data on these particular ternary alloys appears to be most useful in experimentally determining which of these models is most accurate for the III–V semiconductors.

REFERENCES

1. L. Nordheim, *Annalen der Physik* **I.9** 607 and **II.9**, 641 (1931).
2. H. Brooks, Unpublished results.
3. J. J. Tietjen and L. R. Weisberg, *Appl. Phys. Lett.* **7**, 261 (1965).
4. L. Makowski and M. Glicksman, *J. Phys. Chem. Sol.* **34**, 487 (1973).
5. M. Glicksman, R. E. Enstrom, S. A. Mittleman and J. R. Appert, *Phys. Rev B* **9**, 1621 (1974).
6. Y. Takdea, A. Sasaki, Y. Imamura and T. Takagi, *J. Appl. Phys.* **47**, 5405 (1976).
7. J. W. Harrison and J. R. Hauser, *J. Appl. Phys.* **47**, 292 (1976).
8. J. W. Harrison and J. R. Hauser, *Phys. Rev. B* **9**, 5347 (1976).
9. J. R. Hauser, M. A. Littlejohn and T. H. Glisson, *Appl. Phys. Lett.* **28**, 458 (1976).
10. M. A. Littlejohn, J. R. Hauser and T. H. Glisson, *Appl. Phys. Lett.* **30**, 242 (1977).
11. C. J. Neuse, *J. Elec. Mat.* **6**, 253 (1977).
12. W. Fawcett, A. D. Boardman and S. Swain, *J. Phys. Chem. Solids* **31** 1963 (1970).
13. A. E. Asch and G. L. Hall, *Phys. Rev.* **132**, 1047 (1963).
14. D. K. Ferry, Unpublished results.
15. J. C. Phillips, *Rev. Mod. Phys.* **42**, 317 (1970).
16. J. A. Van Vecten and T. K. Bergstresser, *Phys. Rev. B* **1**, 3351 (1970).
17. M. Altarelli, *Solid State Commun.* **15**, 1607 (1974).
18. D. E. Aspnes, *Phys. Rev. B* **14**, 5331 (1976).
19. M. A. Littlejohn, J. R. Hauser and T. H. Glisson, *Appl. Phys. Lett.*, to be published.
20. H. Kroemer, *CRC Crit. Rev. in Sol. State Sci.* **5**, 555 (1975).
21. J. A. Van Vecten, *Phys. Rev.* **182**, 891 (1969).
22. C. Kittel, *Introduction to Solid-State Physics*, 4th Edn, p. 279. Wiley, New York (1971).
23. J. C. Phillips, *Bonds and Bands in Semiconductors*, p. 22. Academic Press, New York (1973).
24. B. G. Basch and R. W. Englemann, *Gunn-effect Electronics*. Wiley, Halstead Press, New York (1975).
25. K. Lehovec and R. Zuleeg, *Solid-St. Electron.* **13**, 1415 (1970).
26. S. Asai, S. Okazaki and H. Kodera, *Solid-St. Electron.* **19**, 461 (1976).

APPENDIX A

Ternary scattering potential from the heteropolar crystal energy

The heteropolar crystal energy in a binary $A^{III}B^{V}$ semiconductor is given in r.m.k.s. units by [15, 16]

$$C_{AB} = \frac{b}{4\pi\epsilon_0}\left[\frac{Z_A}{r_A} - \frac{Z_B}{r_B}\right]\exp(-k_s R), \tag{A1}$$

where Z_A and Z_B are the valence numbers (3 and 5, respectively), r_A and r_B are the covalent radii, $R = 0.5(r_A + r_B)$ is the A–B bond length, and k_s is the Thomas–Fermi screening wave number. The factor b accounts for the fact that the Thomas–Fermi approximation overestimates screening for small interatomic distances [16]. The Thomas–Fermi wave number is given in r.m.k.s. units by [22]

$$k_s^2 = \frac{1}{4}\left(\frac{\pi}{3}\right)^{1/3}\frac{a_B}{n_0}, \tag{A2}$$

where n_0 is the valence electron density [15] and a_B is the Bohr radius. The valence electron density is then given by

$$n_0 = \frac{32}{a_0^3}, \tag{A3}$$

where a_0 is the zincblende lattice constant.

If the binary materials $A^{III}C^{V}$ and $B^{III}C^{V}$ are alloyed to form $A^{III}_{1-x}B^{III}_{x}C^{V}$ and it is assumed that the A–C and B–C bond lengths are equal, then the fluctuations in the heteropolar energy in the alloy can be expressed as [16]

$$\Delta C = |C_{AC} - C_{BC}| \tag{A4}$$

or

$$\Delta C = \frac{bZ}{4\pi\epsilon_0}\left[\frac{1}{r_A} - \frac{1}{r_B}\right]\exp(-k_s R_A),$$

where Vegard's law is assumed to apply to both a_0 and R_A. Thus

$$\begin{aligned} a_0 &= (1-x)a_{AC} + x a_{BC} \\ R_A &= \frac{1}{2}[r_C + x r_B + (1-x)r_A] \end{aligned} \tag{A5}$$

If this fluctuation is taken to be the scattering potential, then $\Delta U_{EN} = \Delta C$, according to the electronegativity theory of Phillips [15, 16]. Equations (1)–(5) are used to calculate the entries in Table 1. Here the rationalized covalent radii given by Phillips [23] have been used in the calculations.

APPENDIX B

Quaternary alloy scattering rate

For a quaternary III–V alloy, $A^{III}_{1-x}B^{III}_{x}C^{V}_{1-y}D_y^{V}$, the virtual crystal potentials for group III and V elements, respectively, are [1]

$$\begin{aligned} U_{III} &= (1-x)U_A + xU_B \\ U_V &= (1-y)U_C + yU_D, \end{aligned} \tag{B1}$$

where U_A, U_B, U_C and U_D are the atomic crystal potentials of each element. If the A and B atoms are randomly placed on the group III sites and the B and C atoms are similarly placed on Vsites, the scattering rates due to potential flucutations of both III and V sites will be proportional to the square of the matrix elements and the probability of occurrence of each species of atom. The probabilities for occurrence in a random crystal are $(1-x)$, x, $(1-y)$, and y for A, B, C and D atoms, respectively. The matrix elements are given by

$$|m_i|^2 = \left|\int \psi^* \Delta U_i \psi \, d\bar{r}\right|^2 \tag{B2}$$

where $\Delta U_i = U_{III} - U_i$ for $i = A$ or B, and $\Delta U_i = U_V - U_i$ for $i = C, D$. Thus, the total scattering rate for the quaternary alloy is given by

$$\frac{1}{\tau_{QA}} \sim x(1-x)|M_{III}|^2 + y(1-y)|M_V|^2 \tag{B3}$$

with

$$|M_{III}|^2 = \left| \int \psi^*(U_A - U_B)\psi \, d\bar{r} \right|^2$$
$$|M_V|^2 = \left| \int \psi^*(U_C - U_D)\psi \, d\bar{r} \right|^2. \tag{B4}$$

If $U_A - U_B$ is regarded as the change in group III potential with grou V atom fixed, and $U_C - U_D$ is regarded as the change in group V potential with group III atom fixed, then the composition weighted averages for $U_A - U_B$ and $U_C - U_D$ are

$$U_B - U_A = (1-y)(U_{BC} - U_{AC}) + y(U_{BD} - U_{AD})$$
$$U_C - U_D = (1-x)(U_{BD} - U_{BC}) + x(U_{AD} - U_{AC}). \tag{B5}$$

Here $(U_{BC} - U_{AC})$ represents the difference in the effective potential for electrons with either group B or group A atoms on group III sites with a C atom definitely on a group V site, and so on for the other three terms.

By substitution of eqn (5) into eqn (4) and neglecting the "overlap" integrals one obtains

$$\frac{1}{\tau_{QA}} = K[x(1-x)y^2|M_{ABD}|^2 + x(1-x)(1-y)^2|M_{ABC}|^2 + y(1-y)x^2|M_{BCD}|^2 + y(1-y)(1-x)^2|M_{ACD}|^2] \tag{B6}$$

where

$$|M_{ABD}|^2 = \left| \int \psi^*(U_{BD} - U_{AD})\psi \, d\bar{r} \right|^2$$

with analogous expressions for the remaining matrix elements. Here the factor K is a quaternary material constant. If the Mott-inner potential model is used[8], the expression for the scattering rate for the quaternary alloy becomes

$$\frac{1}{\tau_{QA}} = \frac{3\pi}{8\sqrt{(2)}} \frac{(m^*)^{3/2}}{\hbar^4} \gamma(\epsilon) \frac{d\gamma}{d\epsilon} \Omega |\Delta U_Q(x, y)|^2, \tag{B7}$$

with

$$|\Delta U_Q(x,y)|^2 = x(1-x)y^2|\Delta U_{ABD}|^2 + x(1-x)(1-y)^2|\Delta U_{ABC}|^2 + y(1-y)x^2|\Delta U_{BCD}|^2 + y(1-y)(1-x)^2|\Delta U_{ACD}|^2.$$

Here the ΔU's on the r.h.s. of eqn (7) are ternary scattering potentials. For example, ΔU_{ABD} is the scattering potential of the ternary $A_{1-x}B_xD$ and ΔU_{BCD} is the scattering potential of the ternary $BC_{1-y}D_y$. In addition, each material parameter in eqn (7) is a material parameter of the quaternary alloy, which can be estimated from binary and ternary material parameters by the interpolation procedures previously described[10].